Available online at www.sciencedirect.com
ScienceDirect
Procedia Engineering 97 (2014) 994 – 1003
Procedia Engineering
www.elsevier.com/locate/procedia

12th GLOBAL CONGRESS ON MANUFACTURING AND MANAGEMENT, GCMM 2014

Analysis of tribological behavior of aluminium/B_4C composite under dry sliding motion

Siddhartha Prabhakar. N[a]*, Radhika. N[b], Raghu.R[c]

[a,b,c]*Dept of Mechanical Engineering, Amrita Vishwa Vidyapeetham, Ettimadai, Coimbatore, India – 641112*

Abstract

This present study deals with the fabrication of aluminium/boron carbide metal matrix composite and investigation on its tribological behavior. The composite incorporated with 5 wt% of boron carbide particles with an average size 33µmwas fabricated through stir casting process. The microstructure of this composite was examined and uniform distribution of reinforced particles in the matrix was observed. Wear experiments were conducted on pin-on-disc tester based on Taguchi's L_{27} orthogonal array using three process parameters such as applied load, sliding velocity and distance; each varied for three levels. Loads of 10 N, 20 N, 30 N; velocities of 1 m/s, 2 m/s, 3 m/s and distances of 1000 m, 1500 m, 2000 m were considered for analyzing the wear behavior of composite. Optimum parameters were found out using Signal-to-Noise ratio by choosing 'Smaller-the-better' characteristics for wear rate and coefficient of friction. Influence of individual parameter and their interactions on the responses was predicted using Analysis of Variance. Results depicted that both wear rate and coefficient of friction increases with load and decreases with velocity and distance. Worn out surfaces of the composite specimen were analyzed using Scanning Electron Microscope for predicting the wear mechanism. It was observed that, severe delamination occurred as applied load increased from 10 N to 30 N. This tribological analysis can be utilized to replace the conventional automotive materials with aluminium metal matrix composites having better wear characteristics.

Selection and peer-review under responsibility of the Organizing Committee of GCMM 2014

Keywords: Aluminium Metal Matrix Composite; Adhesive wear; Coefficient of friction; Signal-to-Noise ratio; Analysis of Variance; Scanning Electron Microscope.

1. Introduction

General engineering materials have limitations in achieving optimum levels of strength, stiffness, density, toughness and wear resistance. The composite materials give engineers the opportunity to tailor the material properties

* Corresponding author. Tel.: +91-944-057-7696.
E-mail address: siddhu.nandamuri@yahoo.com

Selection and peer-review under responsibility of the Organizing Committee of GCMM 2014
doi:10.1016/j.proeng.2014.12.376

according to their needs. These composites were endowed with good tribological properties due to the presence of hard reinforcements. Aluminium Metal Matrix Composites (AMMCs) gained importance due to their enhanced tribological properties that replaces their monolithic counterparts primarily in automotive, aerospace and energy applications [1]. Their resistance to wear added with strength and modulus characteristics made them crucial for many engineering situations, where sliding contact can be expected. Besides the work on abrasive wear behavior, an extensive review on dry sliding wear characteristics of aluminium alloy based composites was carried out[2,3]. Reviews were indicating the tribology of AMMCs as a function of the applied load, reinforcement volume fraction, sliding velocity, distance and nature of the reinforcing phase [4,5,6].Interaction between load and sliding velocity over wear of a material was reported by several researchers [6,7]. High wear resistance of particulate reinforced AMMCs was due to the ceramic particle content, which protects the metal matrix from wear. For AMMCs reinforced with ceramic particles, increased particle content enhances the wear resistance [8]. Investigation on influence of process parameters on hybrid AMMCs was successfully done using Taguchi's technique [9]. Extensive usage of particle reinforced AMMCs in automotive and aircraft industries was found for pistons, brake pads, etc. where tribological properties of the material should be taken care [10]. The type of reinforcement also has a significant role in determining the mechanical and tribological properties of the composites. The effect of different type of reinforcements such as Silicon Carbide (SiC) whisker, Alumina (Al_2O_3) fiber and SiC particle on the properties of Metal Matrix Composites (MMCs), fabricated by powder metallurgy has been investigated. It was found that, there existed a strong dependence on the kind of reinforcement and its volume fraction. The results revealed that particulate reinforcement was most beneficial for improving the wear resistance of MMCs [11]. While SiC and Al_2O_3 reinforced AMMCs were the most studied, limited research have been conducted on dry sliding tribology of aluminium – Boron Carbide (B_4C) composites.

Based on the above study, to enhance the wear properties for automotive applications, LM14 aluminium alloy matrix reinforced with 5 wt% of B_4C particles was produced by stir casting route. The composite was investigated for its tribological behavior by evaluating the wear rate and coefficient of friction using Design of Experiments (DOE).

2. Taguchi's technique

The main trust of Taguchi's technique was the use of parameter design that determines the parameter settings which produces the best levels of a quality characteristic with minimum variation. Taguchi's technique was best suited for manufacturing problems [12]. This methodology acquires data in a controlled way through limited number of experiments which gives the accurate nature of the process. Further depending on the number of factors, interactions and their level, an orthogonal array was selected. Taguchi method follows Signal-to-Noise (S/N) ratio as the quality characteristic of choice.

3. Material selection

LM14 aluminium alloy having density of 2.72 gm/cm^3 and prominent properties like weight, toughness, heat conduction etc. was chosen as the base matrix due to its usage in automotive pistons. In the aim of increasing the wear resistance of this piston alloy, B_4C particles of 33μm size was selected as reinforcement. This B_4C has lower density (2.52 gm/cm^3), higher hardness relative to SiC and Al_2O_3, excellent chemical and thermal stability [13], which makes it as a suitable reinforcement to improve the wear performance of the alloy. The spectroscopy analysis was carried out for LM14 aluminium alloy and its chemical composition was given in Table 1.

Table 1. Chemical composition of LM14 aluminium alloy.

Composition	Si	Fe	Cu	Mn	Mg	Cr	Ni	Sn	Ti	Pb	Ca	Al
%	0.237	0.323	3.46	0.225	1.28	0.0011	2.51	0.061	0.0243	0.0307	0.0071	Balance

4. Synthesis of composite

Stir casting process was used for the fabrication of the composite due to its cost effectiveness [14]. Initially matrix material was fed into the graphite crucible and melted in an electric resistance furnace. The melting of the alloy takes place in an inert gas atmosphere, which avoids chemical reaction and produces a sound casting. After attaining the molten metal condition, preheated reinforcements were added gradually to the molten metal and stirred continuously at 300 rpm for 5 minutes to ensure uniform dispersion of reinforcement particles in molten metal. The molten metal was then poured at the temperature of 760 ºC into preheated (300 ºC) steel mold of dimensions 25 x 25 x 200 mm and allowed to solidify. The pictorial representation of the entire fabrication process was shown in Fig 1.

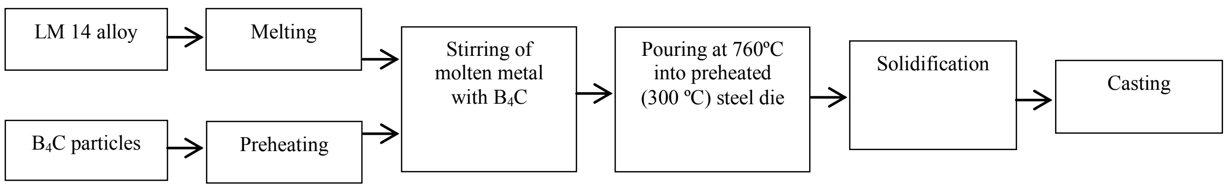

Fig. 1. Pictorial representation of fabrication of MMC.

5. Microstructural investigation

The composite specimen was polished mechanically for removing debris present on the surface using emery paper of grades 1-4. Before the application of Keller's reagent for etching, velvet polishing and diamond polishing were done to ensure fine finishing. Then the microstructure of the specimen was taken using Zeiss Axiovert 25 CA Inverted Metallurgical Microscope.

6. Design of experiments

Plan of experiments was done using Taguchi's technique and L_{27} orthogonal array was opted for getting the best results with minimum number of experiments (Table 2). Wear rate of the specimen and the average coefficient of friction were the two responses evaluated using S/N ratio and Analysis of Variance (ANOVA). Experiments were conducted by considering three parameters; applied load, sliding velocity and sliding distance, each of these varied for three levels (Table 2).

Table 2. Process parameters and their levels.

Levels	Applied load (*N*)	Sliding velocity(*m/s*)	Sliding distance (*m*)
1	10	1	1000
2	20	2	1500
3	30	3	2000

7. Adhesive wear test

The cast component was machined into rectangular specimen of 12x12x35mm dimensions by milling. Dry sliding wear tests on those specimens were conducted using a DUCOM make pin-on-disc tester (Fig.2(a)) as per L_{27} orthogonal array [15]. Test pins (12x12x35mm) (Fig. 2(b)) were held against a rotating steel disc (EN-32) of hardness HRC65. Track diameter of 90 mm was made constant for all the experiments. Load was applied on the cantilever beam that exerts equal amount of force on the specimen for contact with the counter face. The wear of the specimen was monitored using a Linear Variable Differential Transducer (LVDT) which was attached to the lever of the machine. The applied load forces the pin to be in contact with the disc. Wear mechanism of the surface leads to the minor change in the dimensions of the pin, thus displacing the lever arm. This displacement of the lever arm gives input to LVDT for measuring the respective wear. Before and after the experiment, specimen was cleaned properly and weighed using a microbalance of least count 0.1mg. The mass loss of the specimen was calculated and converted into volume loss and thereby to wear rate respectively. The coefficient of friction between the pin and the rotating disc was measured using friction sensors under regular intervals and was recorded by the WINDUCOM software. Taking the average of those values gives average coefficient of friction.

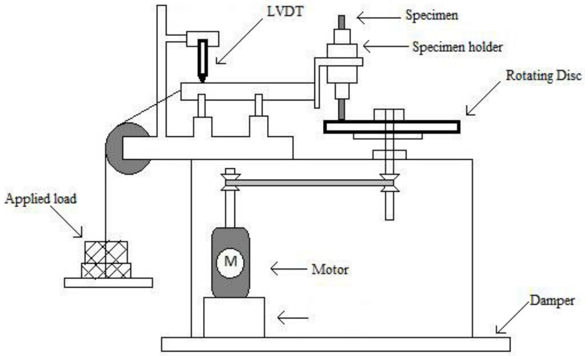

Fig. 2(a). Pin-on-disc tester.

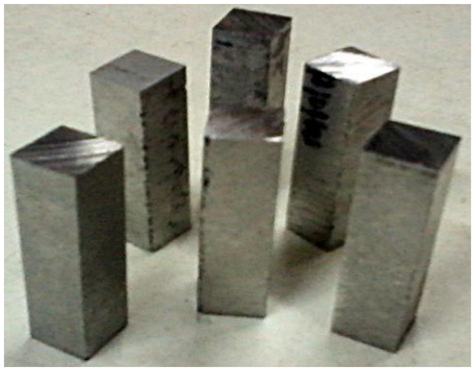

Fig. 2(b). Test composite pins for wear experiments.

8. Results and discussions

Microstructure of the composite specimen and its tribological behavior were evaluated. Scanning Electron Microscope (SEM) analysis was conducted on the worn-out surfaces for determining the wear mechanisms under varying load conditions. These results were explained in brief in the subsequent sections.

8.1. Microstructural evaluation

Evaluation of the microstructure was done to observe the dispersion of particles in the matrix. A typical micrograph of the composite was shown in Fig. 3, which displays the uniform distribution of particles in the matrix. Stirring of molten metal in inert atmosphere at 300 rpm might be the reason for this uniform distribution.

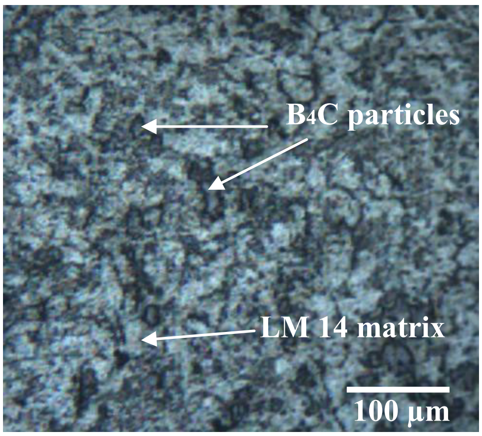

Fig. 3. Micrograph of the composite specimen.

8.2. Tribological behavior

Tribological behavior of the composite, i.e. wear rate and coefficient of friction was evaluated. Table 3 shows the results and their corresponding S/N ratios.

Table 3. L_{27} orthogonal array.

S.No	Process Parameters			Wear Rate(mm^3/m)	S/N ratio (db)	Coefficient of Friction	S/N ratio (db)
	Load (N)	Velocity (m/s)	Distance (m)				
1	10	1	1000	0.002861	50.8696	0.313	10.0891
2	10	1	1500	0.002396	52.4103	0.249	12.0760
3	10	1	2000	0.002665	51.4861	0.183	14.7510
4	10	2	1000	0.002343	52.6046	0.245	12.2167
5	10	2	1500	0.002242	52.9873	0.221	13.1122
6	10	2	2000	0.001944	54.2261	0.160	15.9176
7	10	3	1000	0.002200	53.1515	0.224	12.9950
8	10	3	1500	0.001956	54.1726	0.204	13.8074
9	10	3	2000	0.001896	54.4432	0.169	15.4423
10	20	1	1000	0.002967	50.5536	0.337	9.4474
11	20	1	1500	0.002142	53.3836	0.271	11.3406
12	20	1	2000	0.002725	51.2927	0.216	13.3109
13	20	2	1000	0.002690	51.4050	0.306	10.2856
14	20	2	1500	0.002345	52.5971	0.271	11.3406
15	20	2	2000	0.001838	54.7131	0.209	13.5971
16	20	3	1000	0.002500	52.0412	0.283	10.9643
17	20	3	1500	0.002253	52.9448	0.263	11.6009
18	20	3	2000	0.002096	53.5722	0.193	14.2889
19	30	1	1000	0.004165	47.6077	0.369	8.6595
20	30	1	1500	0.003535	49.0322	0.312	10.1169
21	30	1	2000	0.003266	49.7197	0.276	11.1818
22	30	2	1000	0.003684	48.6736	0.348	9.1684
23	30	2	1500	0.003161	50.0035	0.306	10.2856
24	30	2	2000	0.002541	51.8999	0.277	11.1504
25	30	3	1000	0.003520	49.0691	0.312	10.1169
26	30	3	1500	0.002503	52.0308	0.240	12.3958
27	30	3	2000	0.002415	52.3417	0.261	11.6672

8.3. Analysis of signal-to-noise ratio

S/N ratio in Taguchi's technique indicates the ranking of parameters based on their influence. Response table for S/N ratios of wear rate and coefficient of friction was shown in Table 4 & 5. 'Smaller-the-better' characteristic was taken for this analysis. The difference between the peak values gives the delta value of corresponding parameter. Ranking was allotted in the descending order of the delta value. Considering the wear rate, load was the major parameter which had its influence followed by distance and velocity (Table 4). Last row of Tables 4 & 5 indicates the corresponding ranking of parameters.

Table 4. Response table for S/N ratios - wear rate.

Level	Load (N)	Velocity (m/s)	Distance (m)
1	52.93	50.71	50.66
2	52.50	52.12	52.17
3	50.04	52.64	52.63
Delta	2.89	1.93	1.97
Rank	1	3	2

Taking coefficient of friction into account, distance was ranked first for its influence on it, followed by applied load and the sliding velocity (Table 5). Presence of hard reinforcements could be the reason for the rank of distance.

As the distance increases, the reinforcement particles which protrude out of the surface get fractured, thus increasing the contact area between the sliding surfaces which in turn reduces the friction.

Table 5. Response table for S/N ratios – coefficient of friction.

Level	Load*(N)*	Velocity *(m/s)*	Distance*(m)*
1	13.38	11.22	10.44
2	11.8	11.90	11.79
3	10.53	12.59	13.48
Delta	2.85	1.37	3.04
Rank	2	3	1

8.4. Influence of parameters on the responses

Effect of process parameters on wear rate and coefficient of friction was evaluated. Mean plot indicated in Fig 4(a) & 5(a) shows the trend of the corresponding responses. Fig 4(b) & 5(b) shows the optimal level of parameters using S/N ratios. Influence of parameters on the responses was discussed in detail in the later sections.

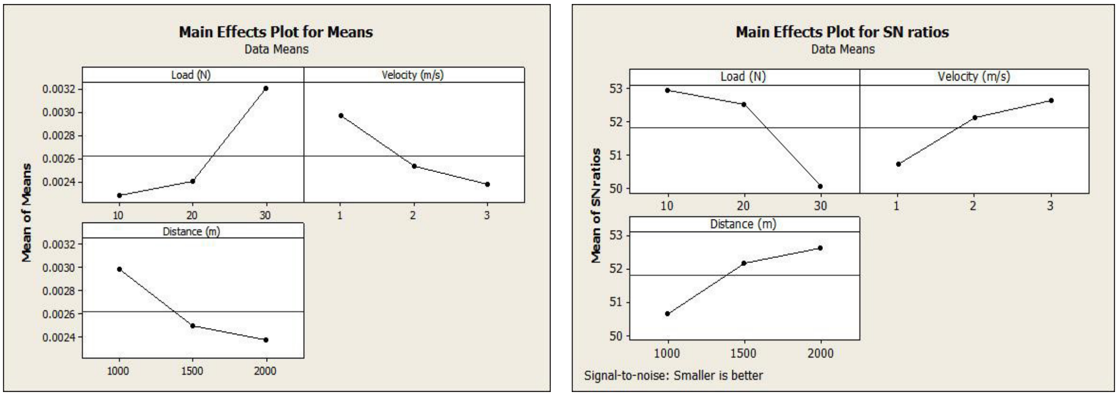

Fig. 4. (a) Main effect plot for means – wear rate. (b) Main effect plot for S/N ratios – wear rate.

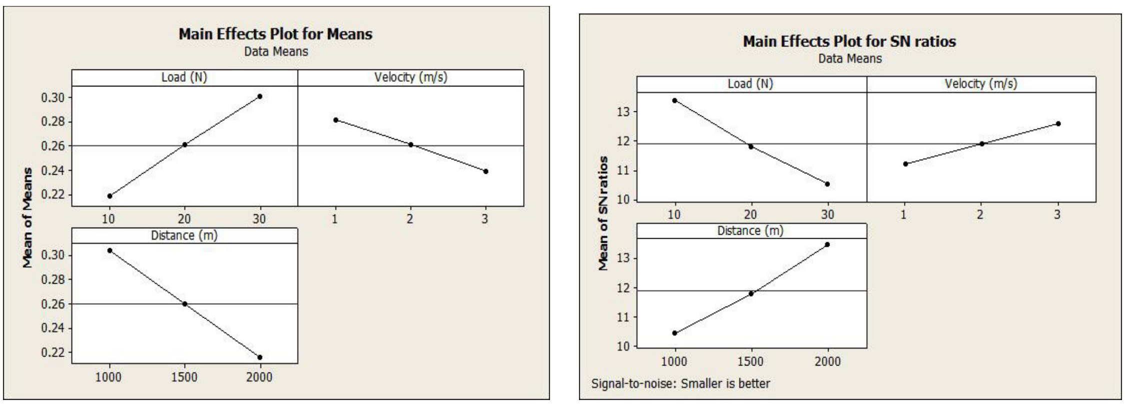

Fig. 5. (a) Main effect plot for means – coefficient of friction. (b) Main effect plot for S/N ratios – coefficient of friction.

8.4.1. Effect of load

From graph (Fig 4(a) & 5(a)), it was observed that both wear rate and coefficient of friction increases when applied load increases. From 10 N to 20 N, marginal increase of wear rate was observed, whereas drastic increase from 20 N to 30 N. This trend can be attributed to the plastic deformation of the material. At low loads (10 N and 20 N), temperature rise over the sliding surface had less effect on the plastic deformation. Increased load (30 N) on the specimen leads to increase in temperature over the sliding surface even at low sliding velocities. Due to this high temperature, plastic deformation of the surface occurred leading to the adhesion of pin surface onto the disc. This adhesion results in more material removal, thereby drastically increasing the wear rate [16]. Increased coefficient of friction can be related to the fragmentation of oxide layer. The B_4C particles which were pulled out during sliding reacts with the atmosphere at low loads, forming the B_2O_3 layer. This boron oxide layer was greatly influenced by the temperature over the surface of the contact. At low velocity, as the applied load increases, delamination of this oxide layer occurs, forming scratches and grooves on the pin surface. This increases the friction between the sliding surfaces [17].

8.4.2. Effect of distance

As distance increases, both wear rate and coefficient of friction were observed to be decreasing. This decreasing trend interprets the inverse relation as indicated in the graph (Fig 4(a)& 5(a)). Wear rate decreased to a large extent from 1000 m to 1500 m when compared with the wear rate between 1500 m to 2000 m. This behavior can be supported by the presence of hard reinforcements that act as sharp asperities on the surface of the composite specimen. Initially at low distance, reinforcement particles which protrude out of the composite surface decrease the contact area between the specimen and the disc, which in turn increases the wear rate and friction. As the distance increases, these asperities get compacted between the sliding surfaces and becomes blunt, thereby considerably increasing the contact area between the two sliding surfaces [18]. This could be the reason for improvised wear behavior under high distance.

8.4.3. Effect of velocity

The responses were observed to be decreasing with increasing velocity (Fig 4(a) & 5(a)). This can be supported by the formation of tribo layer. Aluminium has an inherent property of forming an oxide layer on its outer periphery. When sliding at high velocity, the temperature increases over the contact surface, making the material to oxidize. This phenomena leads to the transferring of materials, forming Mechanically Mixed Layer (MML), also called tribo layer. As the velocity increases, this tribo layer will act as a barrier or lubricant between the two surfaces decreasing the wear rate and the coefficient of friction [19]. The optimum parameters for enhancing the tribological behavior of the composite were low load (10 N), high sliding velocity (3 m/s) and maximum distance (2000 m) (Fig. 4(b) & 5(b)).

8.4.4. Comparison plot for wear rate

The wear rate of the composite specimen on varying load (10 N, 20 N, 30 N) was compared in the graph (Fig 6). Considering the sliding velocity of 2 m/s and distance of 1500 m as constant, wear rate was calculated for all the three levels of load. These values were compared on a single scale which interprets the directly proportional relation between applied load and wear rate.

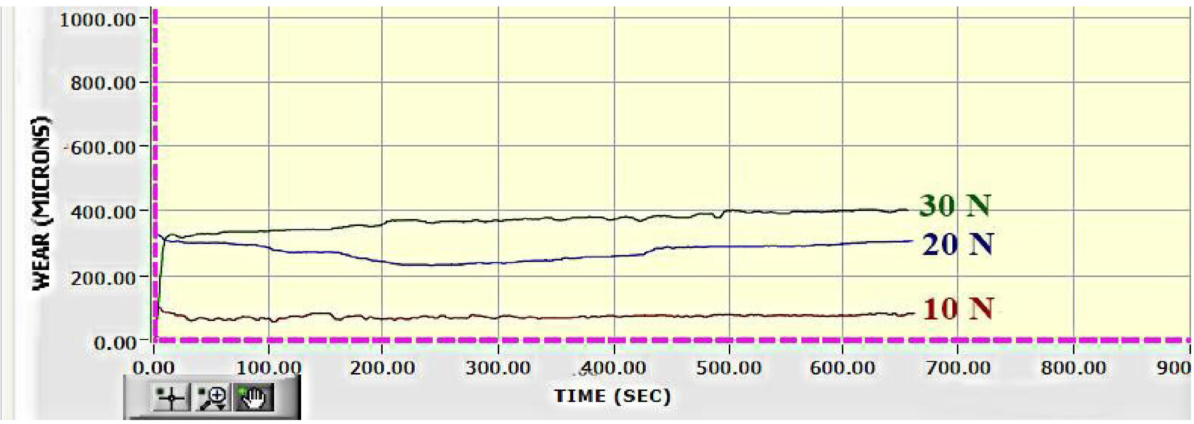

Fig. 6. Comparison plot of wear rate for varying load.

8.5. Analysis of variance

ANOVA investigates which of the process parameters and their interactions significantly affect the performance characteristics. ANOVA for wear rate and coefficient of friction was indicated in Table 6 & 7 respectively. This analysis was carried out for a level of significance 5%, i.e., for a level of confidence 95%. 'P' value, less than 0.05 for a particular parameter, indicates that it has the major effect on the responses. Last column in Table 6 & 7 shows the percentage effect of individual parameters and interactions on the responses.

Table 6. ANOVA for wear rate.

Source	DF	Seq SS	Adj SS	Adj MS	F	P	Pct*(%)*
Load (*N*)	2	0.0000045	0.0000045	0.0000023	96.42	0.000	47.4
Velocity (*m/s*)	2	0.0000017	0.0000017	0.0000009	36.76	0.000	18.9
Distance (*m*)	2	0.0000019	0.0000019	0.0000010	40.57	0.000	22
Load*Velocity	4	0.0000002	0.0000002	0.0000001	2.16	0.164	2.2
Load*Distance	4	0.0000005	0.0000005	0.0000001	4.94	0.027	5.4
Velocity*Distance	4	0.0000003	0.0000003	0.0000001	3.60	0.058	3.2
Error	8	0.0000002	0.0000002	0.0000000			2.2
Total	26	0.0000093					

From Table 6, it was observed that the major controlling parameter for wear rate was load (47.4%) followed by distance (22%) and velocity (18.9%). Among the interactions, load with distance accounts for highest percentage (5.4%), showing their influence on the wear rate. Pooled error accounts for only 2.2%. Hence load was the major process parameter to be considered in this wear process due to its significant influence.

Table 7. ANOVA for coefficient of friction.

Source	DF	Seq SS	Adj SS	Adj MS	F	P	Pct*(%)*
Load (*N*)	2	0.0298650	0.0298650	0.0149325	108.22	0.000	37.7
Velocity (*m/s*)	2	0.0078983	0.0078983	0.0039491	28.62	0.000	10.0
Distance (*m*)	2	0.0349370	0.0349370	0.0174685	126.60	0.000	44.1
Load*Velocity	4	0.0013373	0.0013373	0.0003343	2.42	0.133	1.7
Load*Distance	4	0.0020279	0.0020279	0.0005070	3.67	0.055	2.6
Velocity*Distance	4	0.0020946	0.0020946	0.0005236	3.80	0.051	2.6
Error	8	0.0011039	0.0011039	0.0001380			1.4
Total	26	0.0792639					

Note: DF-Degrees of Freedom; Seq SS-Sequential Sum of Squares; Adj SS-Adjacent Sum of Squares; Adj MS-Adjacent Mean of Squares; F-Fisher's test; Pct-Percentage.

From Table 7, distance was investigated as the statistically significant parameter having major influence on the response (44.1%). Applied load (37.7 %), followed by sliding velocity (10 %) were the latter parameters. Both load with distance interaction and velocity with distance interaction shows their influence on the coefficient of friction (Pct=2.6%) and pooled error was only of 1.4%.

8.6. Scanning electron microscope analysis

SEM analysis was done on the worn-out specimen for observing the wear mechanism over the surface of the composite. Fig. 7(a-d) displays the worn-out surface of the specimen at various conditions. Material removal with few scratches was observed at low load (10 N) and grooves along the sliding direction were also found to be shallow (Fig. 7(a)), which indicates minimum wear rate. With increase in applied load from 10 N to 20 N (Fig. 7(b)), more grooves with delamination were observed on the surface. From 20 N to 30 N (Fig. 7(c)), depth and also the number of grooves were found to be more indicating the transition of normal wear to severe wear resulting in heavy metal removal rate. The reason behind this wear mechanism was the plastic deformation between the rotating disc and the composite specimen at high load, resulting in high wear rate. This implies the drastic increase of wear rate from 20 N to 30 N in the graph shown in Fig 4(a). As sliding velocity increased from 1 m/s to 3 m/s, formation of MML took place, enhancing the tribological properties and was inferred by comparing Fig. 7(c) & 7(d). At high velocities, the temperature over the sliding surface increases resulting in oxidization of material and thus material transfer occurs between the pin and counterface which leads to the formation of MML. This layer helps in achieving good tribological properties over high velocities [20].

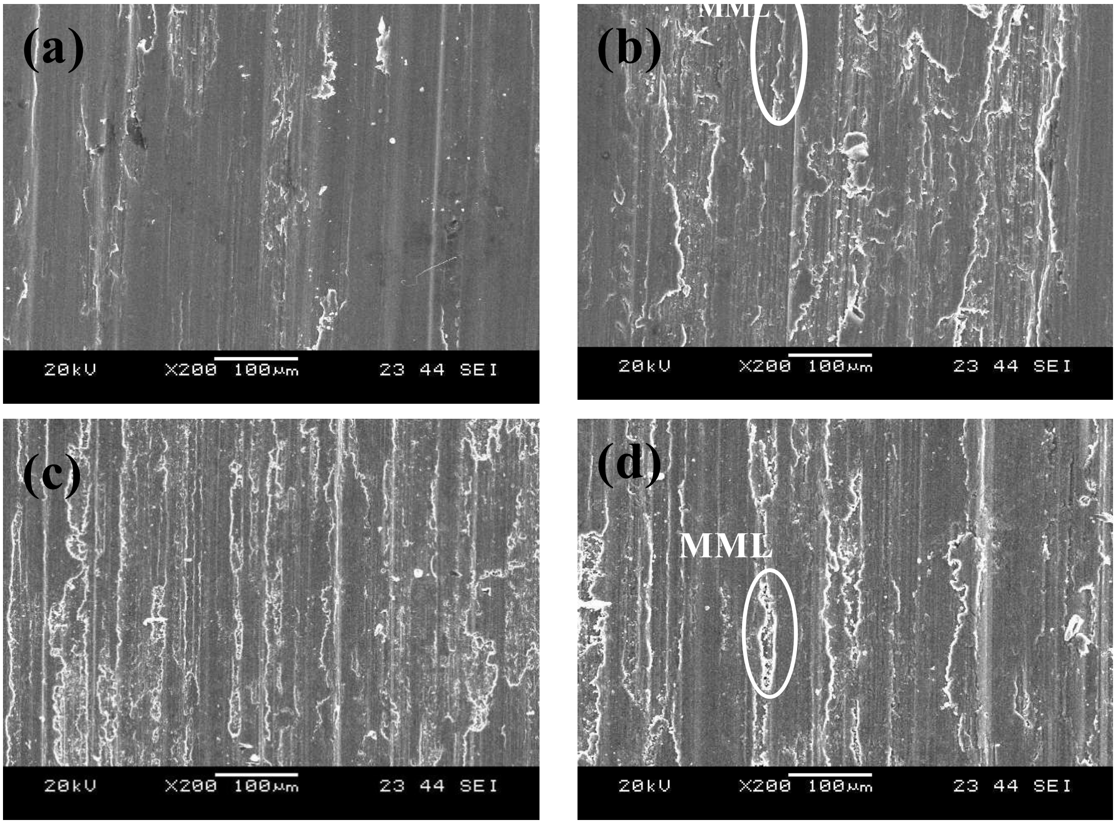

Fig. 7. SEM analysis of worn-out specimens at different conditions (a) L=10N, V=1m/s, D=2000m. (b) L=20N, V=1m/s, D=2000m. (c) L=30N, V=1m/s, D=2000m. (d) L=30N, V=3m/s, D=2000m.

9. Conclusion

LM14 aluminium alloy matrix composite reinforced with 5 wt% of B_4C particles was successfully fabricated through stir casting route. Uniform distribution of particles in the matrix was observed by microstructural investigation. Tribological results revealed that wear rate and coefficient of friction has a direct relation with the load, whereas inverse with the sliding speed and distance. Load was the major factor (47.4%) in determining the wear rate followed by distance and sliding velocity whereas distance affects the coefficient of friction to a large extent (44.1%) followed by load and sliding velocity. Optimum conditions for obtaining good tribological characteristics were low load (10 N) along with high sliding velocity (3 m/s) and distance (2000 m). SEM analysis revealed the wear mechanism and the formation of MML at high velocities.

This investigation of tribological behavior can be efficiently used for sorting out the best materials required for the automotive field, where sliding contact is expected. Replacement of conventional automotive parts like pistons, piston liners, brake rotors, cylinder heads etc. with these AMMCs can be done for having a better life of the components.

References

[1] Anandha Moorthy, Dr.N. Natarajan, R. Sivakumar, M. Manojkumar, M. Suresh, Dry sliding wear and mechanical behavior of aluminium/fly ash/graphite hybrid metal matrix composite using taguchi method, Int. J. Modern. Eng. Res.2 (2012) 1224-1230.

[2] A.P. Sannino, H.J. Rack, Dry sliding wear of discontinuously reinforced aluminium composites: review and discussion, Wear. 189 (1995) 1–19.

[3] R. L. Deuis, C. Subramanian, J.M. Yellup, Abrasive wear of aluminium composites – a review, Wear.201 (1996) 132–44.

[4] A. Baradeswaran, A. ElayaPerumal, Study on mechanical and wear properties of Al 7075/Al_2O_3/graphite hybrid composites, Compos.56 (2014) 464–471.

[5] A.K. Israa, Studying the effect of reinforcing by SiC_p on the dry sliding wear behavior and mechanical properties of Al-4% Cu matrix alloy, Diyala J. Eng. Sci. 06 (2013) 139-153.

[6] M. Singh, D.P. Mondal, S. Das, Abrasive wear response of aluminium alloy–sillimanite particle reinforced composite under low stress condition, Mater. Sci. Eng. 419 (2006) 59–68.

[7] B. Venkataraman, G. Sundararajan, Correlation between the characteristics of the mechanically mixed layer and wear behaviour of aluminium, Al-7075 alloy and Al-MMCs, Wear. 245 (2000) 22–38.

[8] S. Das, Development of aluminium alloy composites for engineering applications, Trans. Indian Inst. Met. 57 (2004) 325-334.

[9] N. Radhika, R. Subramanian, S. VenkataPrasat, Tribological behaviour of aluminium/alumina/graphite hybrid metal matrix composite using Taguchi's techniques, J. Miner. Mater. Charact. Eng. 10(2011) 427-443.

[10] G. Straffelini, M. Pellizzari, A. Molinary, Influence of load and temperature on the dry sliding behaviour of Al-based metal matrix composites against friction material, Wear. 256 (2004) 754–763.

[11] Ashok. Kr. Mishra, Rakesh Sheokand, Dr.R.K. Srivastava, Tribological behaviour of al-6061/sic metal matrix composite by Taguchi's techniques, Int. J. Sci. Res. Publ. 2 (2012) 2250-3153.

[12] W.H. Yang, Y.S. Tarng, Design optimization of cutting parameters for turning operations based on the Taguchi method, J. of Mater. Process. Technol. 84(1998) 122-129.

[13] C.A.Smith, Discontinuous reinforcements for metal-matrix composites, ASM Handbook, vol.21, Composites, ASM International, 2001.

[14] RabindraBehera, S. Das, D. Chatterjee, G. Sutradhar, Forgeability and machinability of stir cast aluminum alloy metal matrix composites, J. Miner. Mater. Charact. Eng. 10(2011) 923-939.

[15] R. Ipek, Adhesive wear behaviour of B_4C and SiC reinforced 4147 Al matrix composites (Al/B_4C-Al/SiC), J. Mater. Process. Technol. 162–163 (2005) 71–75.

[16] R.N.Rao, S.Das. Wear coefficient and reliability of sliding wear test procedure for high strength aluminium alloy and composite, Mater. Des. 31 (2010) 3227–3233.

[17] M. Uthayakumar, S. Aravindan, K. Rajkumar, Wear performance of Al–SiC–B_4C hybrid composites under dry sliding conditions, Mater. Des. 47 (2013) 456–464.

[18] L. Zhang, X.B. He, X.H.Qu, B.H. Duan, X. Lu, M.L. Qin, Dry sliding wear properties of high volume fraction SiC_p/Cu composites produced by pressureless infiltration, Wear. 265 (2008) 1848–1856.

[19] Ferhat Gul, Acilar Mehmet, Effect of the reinforcement volume fraction on the dry sliding wear behaviour of Al-10Si/SiC_p composites produced by vacuum infiltration technique, Compos. Sci. Technol.64 (2004) 1959–66.

[20] S.A. Alidokht, A.Abdollahzadeh, H.Assadi, Effect of applied load on the dry sliding wear behavior and the subsurface deformation on hybrid metal matrix composite, Wear. 305(2013)291–298.